Sol-Gel Synthesis and Characterization of Alumina-15%Mullite Composite Nanopowder

A. Sedaghat[a], E. Taheri-Nassaj[b,*], G. Soraru[c], R. Ceccato[c], T. Ebadzadeh[a]

[a] *Department of Ceramic, Material and Energy Research Center, karaj, Iran.*
[b] *Department of Materials Engineering, Tarbiat Modares University, Tehran, Iran.*
[c] *Department of Materials Engineering and Industrial Technology, University of Trento, Trento, Italy.*

ARTICLE INFO

Article history:

Received 11 Dec. 2013
Accepted 11 Jan. 2014
Available online 25 Feb. 2014

Keywords:

Sol–gel processes
Nanocomposites
Al_2O_3

ABSTRACT

Homogeneous distribution of mullite in the matrix of alumina can be obtained through sol-gel method. In this work, nanopowder of alumina-mullite composite was synthesized with high homogeneity and high purity. Aluminum chloride hexahydrate and tetraethyl orthosilicate were used instead of alumina or mullite nanopowder. Studying the simultaneouse thermal analysis (STA) of mullite precursor reveals two endothermic peaks at 145 and 240°C due to dehydration and removal of the molecular water and the chloride component. An exothermic peak is also detected at 855°C. According to the XRD patterns of alumina-15vol.% mullite precursors calcined at different temperatures, crystallization of transitional alumina phases (γ, κ) occurs approximately at 800°C. Then these phases transform to α alumina approximately at 1000°C. XRD patterns of alumina-15%vol. mullite calcined at different temperatures show peaks of mullite related to 1000°C. The specific surface area of this nanopowder calcined at 900°C was calculated to be 120.9±0.5 m^2/g. The nanopowder was observed by TEM.

1. Introduction

Alumina has been used in different applications such as sandblast nozzles, abrasive materials, insulating refractory linings of furnaces, seals , thermocouple wire protection in electrical devices and armors because of its mechanical, physical and chemical properties (high hardness, good wear resistance, high melting point, low thermal conductivity, good electrical and chemical resistance) [1-3]. On the other hand, mullite in the alumina matrix reduces the Young's modulus and thermal expansion coefficient of the composite which leads to better thermal shock resistance [4-6]. Meanwhile, mullite has low toughness and hardness [7]. Small addition of mullite from 5 to 15%vol. is believed to retain the desirable hardness and toughness properties [8].

Several methods can be used to produce fine powder ceramics with high purity [9] such as evaporation, spray drying, freeze drying, hydrothermal technique and hydrolysis and using plasma for powder synthesis. The sol-gel method has thefollowing advantages over the other techniques:

High purity ceramic is obtained because of

Corresponding author:
E-mail address: taheri@modares.ac.ir (Ehsan Taheri-Nassaj).

previous purification procedures such as distillation or recrystalization which are assumed to be essential steps for liquids or alkoxides,

High homogeneity multi-component ceramics and composite ceramics are obtained since the energy and the synthesis temperature is low enough,

It is possible to prepare various special types of materials such as thin films, coatings and fibers because it is very easy to control the reaction conditions [9-11].

Mullite is one of the most extensively studied crystalline phases through Al_2O_3-SiO_2 binary system due to its low thermal expansion, good thermal and chemical stability and high creep resistance [12]. Mullite is extracted from different sources of silica- and alumina-containing materials. Roy [13] first used tetra ethyl orthosilicate (TEOS) and aluminum nitrate nanohydrate (ANN), thereafter it has been used as organic/inorganic source for the synthesis of mullite precursor through sol-gel technique [14-28]. Usually, mullite precursors form t-mullite and Al-Si spinel of varying ratios at 980°C and then complete o-mullite formation at second stage of transformation occur at 1250°C [14].

The aim of this work is to synthesize nanopowder of alumina-mullite composite with high homogeneity and high purity via sol-gel method. Aluminum chloride hexahydrate and tetraethyl orthosilicate were proposed instead of alumina or mullite nanopowder. Then simultaneous thermal analysis, BET technique, XRD and microstructure analysis were performed for the characterization of the nanopowder.

2. Experimental

The alumina-mullite powder was synthesized using $AlCl_3.6H_2O$ (Merck 101084) dissolved in distilled water and TEOS (Sigma-Aldrich 131903) dissolved in absolute ethanol (C_2H_5OH) via sol-gel technique.

Based on the stoichiometric ratio of mullite and its dependence on the desired volume percentage of mullite (0, 15 and 100vol.%), aqueous solution of $AlCl_3.6H_2O$ with the required amount of the alcoholic solution of the TEOS was refluxed at 60°C for 24h. After condensation, the gel was dried at 120°C for 24h and then ground in an agate mortar. The precursors of mullite and alumina-15vol.%mullite were calcined at 400-1600°C for 2h. The rate of heating was chosen to be 5°C/min. Calcined powders were milled using alumina balls and absolute ethanol. The flowchart of the procedure is depicted in Fig1.

Thermogravimetric and differential thermal analyses (TG, DTA) of the mullite precursor gel and of the dried alumina precursor gel were performed using a Netzsh STA 409. TGA/DTA test were done under the condition of flowing air with heating rate of 10°C/min up to 1575°C. XRD was also carried out for phase characterization of the calcined powder using CuKα radiation. Nitrogen adsorption/desorption of the alumina-15vol.% mullite precursor calcined at 900°C was performed on ASAP2010 Micrometrics. Isothermal curves were sketched and specific surface areas were calculated using BET technique. Pore volume and pore size distribution were also obtained from desorption isotherm via analysis of Barret, Joyner and Halenda [29]. For nonporous particles, the mean particle size (d) of the powder can be calculated from its specific surface area using the following equation [29]:

$$d = SF/(SSA \times \tilde{n}) \quad [1]$$

Where SF is the shape factor and equals to 6 for a spherical powder, SSA is the specific surface area and ρ is the apparent powder density [29]. The apparent density of the calcined alumina-15vol.% mullite precursor at 900°C was measured using a helium picnometer (Micromeritics 1035). Microstructure analysis of this powder was carried out by Philips EM208S TEM instrument operating at 100keV.

3. Results and Discussion

Fig 2 presents the curves of DTA and TGA related to the dried gel of alumina precursor (Fig2(a)) and the gel of mullite precursor (Fig2(b)). DTA curve of the dried gel of alumina precursor reveals some endothermic peaks at 220°C, while its TGA curve shows a weight loss around this temperature. According to fig2 (a), the weight loss disappeared around 850°C. Thus, the calcination should be done around 900°C. The DTA curve of the mullite

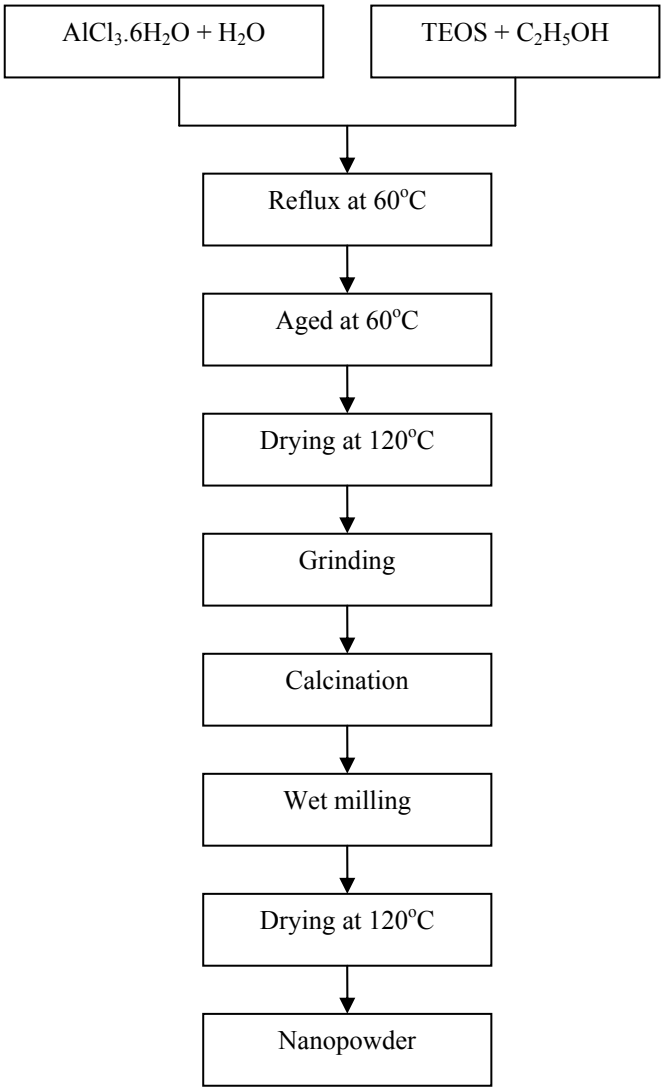

Fig. 1. The flowchart of the alumina–mullite nanopowder processing

precursor gel has two endothermic peaks at 145 and 240°C, whereas the TGA curve is accompanied by a weight loss of about 80% up to 400°C and reveals less change at higher temperatures. This behavior can be attributed to dehydration and removal of the molecular water and the chloride component [30, 31]. DTA curves reveal an exothermic peak at 855°C because of the crystallization of transitional alumina according to the XRD patterns.

Fig 3 presents XRD patterns of (a) the alumina-15vol.% mullite and (b) the mullite precursor calcined at different temperatures (400-1600°C). Figures 3.a and 3.b show the formation of transitional alumina (γ, κ) around 800°C. The XRD patterns of alumina-15vol.% mullite which was calcined at different temperatures (Fig 3. a), shows that the transitional alumina transforms to α-alumina at 1000°C. The mullite peaks are also detected later. Not only mullite is formed at 1000°C (Fig. 3), but also there is some γ-alumina found at 1000 and 1100°C. At higher temperatures, just the mullite peaks can be observed for this sample (Fig 3. b).

Fig 4 presents isotherm patterns of nitrogen adsorption-desorption of alumina-15vol.% mullite precursor calcined at 900°C for 2h. It can be seen that the powder exhibits the Type

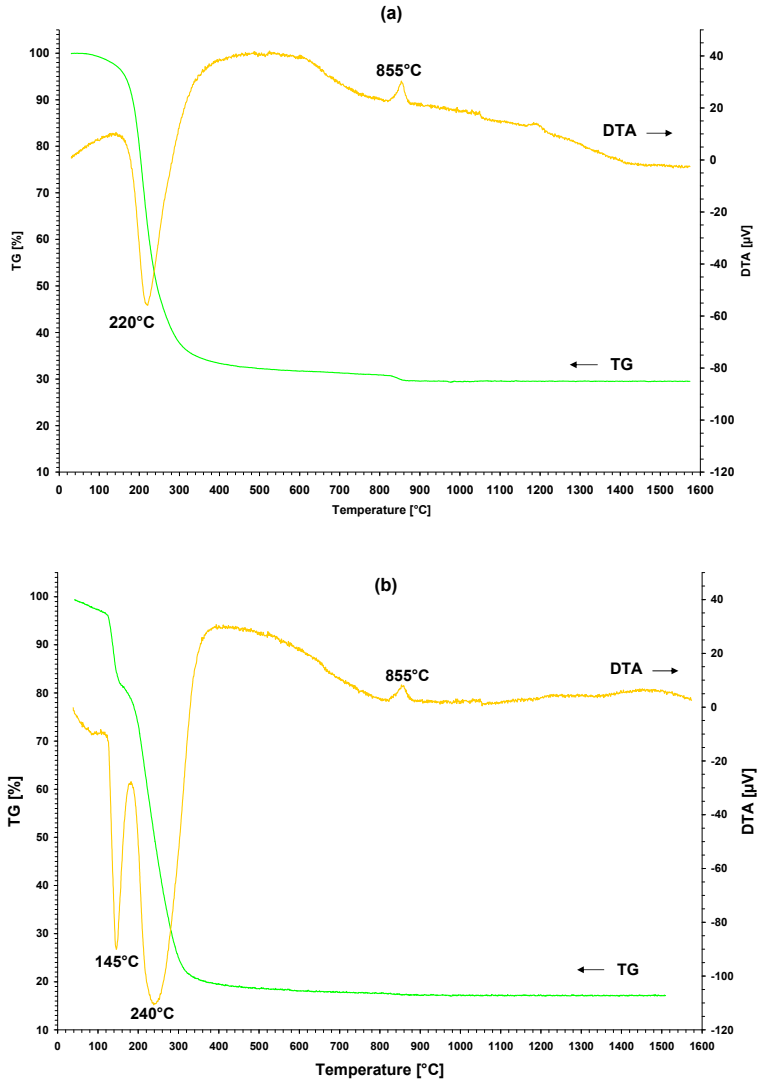

Fig. 2. DTA/TGA for (a) dried gel of alumina precursor and (b) the gel of mullite precursor

IIb group with the presence of mesopores [29]. The shape of the curve and the hysteresis loop (H3-type) can justify the presence of aggregates containing platy particles (alumina shows this typical behavior) with the presence of non-rigid slit-shaped pores which were formed by the aggregates. These platy particles can be observed in the TEM micrograph. Fig 5 shows TEM image of the alumina composite nanopowder heat treated at 900 °C. Most of the particles are platy in shape. Some agglomerates exist in the powders which are attributed to uncontrolled coagulation during synthesis.

The analysis of nitrogen adsorption-desorption is summarized in Table 1. It also shows the density of this sample and its mean particle size calculated from equation (1). The BET surface area and the density were calculated to be 120.922 ± 0.532 m^2/g and 3.637 ± 0.003 g/cm^3, respectively and the mean particle size has the value of 13nm. However, some platelets are observed in Fig5 and equation (2) is applied for equal-sized platelets with thickness of t [32]. This would now be able to explain the apparent discrepancy.

$$SSA = 2/(t \times \tilde{n}) \quad [2]$$

4. Conclusions

In this work, alumina-mullite nanopowder is synthesized by aluminum chloride hexahydrate and tetraethyl orthosilicate via sol-gel technique. The findings can be summarized as below:

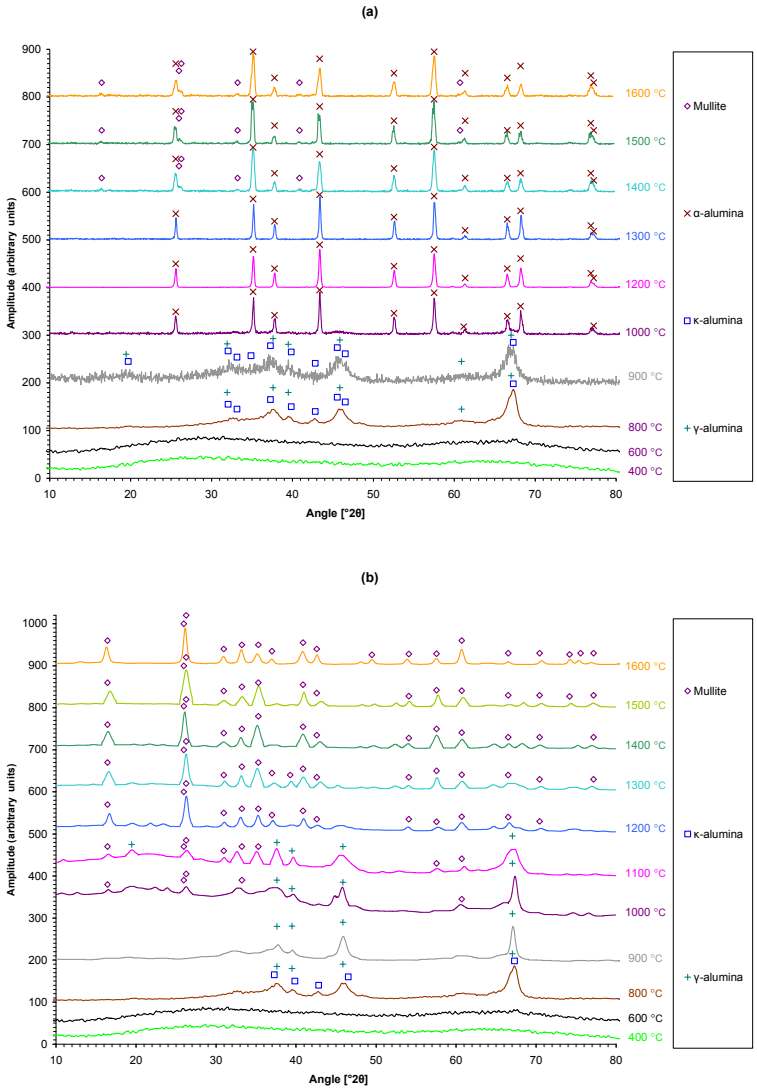

Fig. 3. XRD patterns of (a) the alumina-15vol.%mullite composite and (b) the mullite precursors calcined at different temperatures

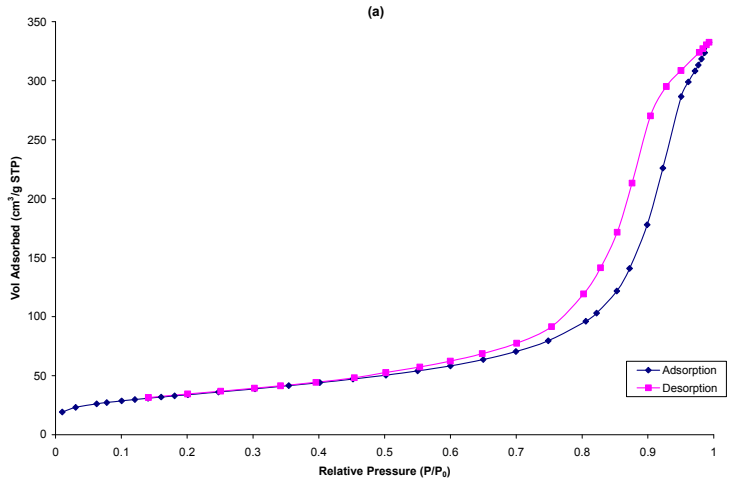

Fig. 4. Nitrogen adsorption–desorption isotherm of the alumina-15%mullite calcined at 900°C for 2h

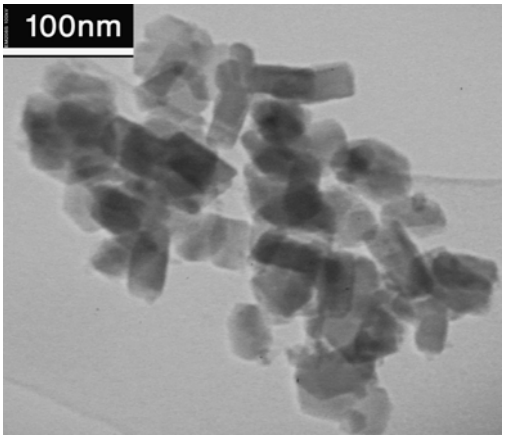

Fig. 5. TEM micrograph (bright field) of the alumina-15vol.% mullite calcined at 900°C for 2h

Table 1. Properties of alumina–15vol.%mullite calcined at 900°C for 2h

BET Surface Area [m²/g]	120.922 ± 0.532
Surface Area of pores [m²/g]	123 .611
Total Pore Volume [cm³/g]	0.513
Mean Pore Diameter (4V/A by BET)	17.018
Density (ρ) [g/cm^3]	3.637 ± 0.003
Mean particle size (d) [nm]	13.128

1. Transitional alumina (γ/κ) is crystallized at 800°C. Itis transformed into α-alumina at 1000°C.
2. The mullite formation starts from 1000°C with the presence of γ-alumina. At 1200°C, it will be completed and there will be no γ-alumina.
3. The BET surface area and the mean particle size of the alumina composite powder, calcined at 900°C for 2h, are found to be 120.9 ± 0.5m^2/g and 13nm, respectively.

References

1. D. W. Richerson, Modern Ceramic Engineering, M. Dekker 1992, pp. 808-823.
2. E. Medvedovski, "Alumina–mullite ceramics for structural applications", Ceram. Int., Vol. 32, 2006, pp. 369–375.
3. H. H. Luo, F. C. Zhang, S. G. Roberts, "Wear resistance of reaction sintered alumina/mullite composites", Mat. Sci. Eng. A, Vol. 478, 2008, pp. 270–275.
4. S. Mezquita, R. Uribe, R. Moreno, C. Baudín, "Influence of mullite additions on thermal shock resistance of dense alumina materials Part 2: Thermal properties and thermal shock behavior", Brit. Ceram. Trans. Vol. 100. No. 6, 2001, pp. 246-250.
5. C. Aksel, "The effect of mullite on the mechanical properties and thermal shock behaviour of alumina–mullite refractory materials", Ceram. Int., Vol. 29, 2003, pp.183–188.
6. F. C. Zhang, H. H. Luo, S. G. Roberts, "Mechanical properties and microstructure of Al_2O_3/mullite composite", J. Mater. Sci. Vol. 42, 2007, pp. 6798–6802.
7. C. Aksel, "The role of fine alumina and mullite particles on the thermomechanical behaviour of alumina–mullite refractory materials", Mater. Lett, Vol. 57, 2002, pp. 708–714.
8. R. Moreno, S. Mezquita, C. Baudín, "Influence of mullite additions on thermal shock resistance of dense alumina materials Part 1: Processing studies", Brit. Ceram. Trans., Vol. 100, No. 6, 2001, pp. 241-245.
9. C. W. Won, B. Siffert, "Preparation by sol-gel method of SiO_2 and mullite ($3Al_20_3.2SiO_2$) powders and study of their surface characteristics by inverse gas chromatography and zetametry", Colloid. Surface. A, Vol. 131, 1998, pp. 161-172.
10. M. Schehl, L. A. Díaz, R. Torrecilla, "Alumina nanocomposites from powder–alkoxide mixtures", Acta Mater. Vol. 50, 2002, pp. 1125–1139.
11. S. Sakka, K. Kamiya, "Glasses from metal alcoholates", J. Non-Cryst. Solids, Vol. 42, 1980, pp. 403-422.
12. T. Ebadzadeh, "Formation of mullite from precursor powders: sintering, microstructure and mechanical properties", Mat. Sci. Eng. A, Vol. 355, 2003, pp. 56-61.
13. R. Roy, "Aids in hydrothermal experimentation. II. Methods of making mixtures for both "dry" and "wet" phase equilibrium studies", J. Am. Ceram. Soc., Vol. 39, 1956, pp. 145-146.
14. A. K. Chakraborty, "Aluminosilicate formation in various mixtures of tetra ethyl orthosilicate (TEOS) and aluminum nitrate

(ANN)", Thermochim. Acta, Vol. 427, 2005, pp. 109–116.
15. H. Schneider, S. Komarneni, Mullite, WILEY-VCH Verlag GmbH and Co. KGaA, Weinheim, 2005, pp. 263-272.
16. M. Yamane, S. Inoue, A. Yasumori, "Sol–gel transition in the hydrolysis of silicon methoxide", J. Non-Cryst. Solids, Vol. 63, 1984, pp. 13.
17. K. Okada, N. Otsuka, "Characterization of spinel phase from SiO_2–Al_2O_3 xerogels and the formation process of mullite", J. Am. Ceram. Soc., Vol. 69, 1986, pp. 652-656.
18. A. K. Chakraborty, D. K. "Ghosh Synthesis and 980°C phase development of some mullite gels", J. Am. Ceram. Soc., Vol. 71, 1988, pp. 978-987.
19. Ch. Sh. Hsi, H. Y. Lu, F. S. Yen, "Thermal behaviour of alumina–silica xerogels during calcinations", J. Am. Ceram. Soc., Vol. 72, 1989, pp. 2208-2210.
20. A. Yasumori, M. Anma, M. Yamane, "Chemical effects of formamide and N,N-dimethylformamide on the formation of alkoxy-derived silica gel", Phys. Chem. Glasses, Vol. 30 1989, pp. 193.
21. T. Heinrich, F. Raether, "Structural characterization and phase development of sol–gel derived mullite and its precursors", J. Non-Cryst. Solids, Vol. 147/148, 1992, pp.152.
22. B. E. Yoldas, "Effect of ultrastructure on crystallization of mullite", J. Mater. Sci., Vol. 27, 1992, pp. 66-67.
23. H. Schneider, B. Saruhan, D. Voll, L. Merwin, A. Sebald, "Mullite Precursor Phases", J. Euro. Ceram. Soc., Vol. 11, 1993, pp. 87.
24. A. K. Chakraborty, "Role of hydrolysis water–alcohol mixture on mullitization of Al_2O_3–SiO_2 monophasic gels", J. Mater. Sci., Vol. 29, 1994, pp. 6131.
25. A. K. Chakraborty, "Effect of pH on 980°C spinel phase—mullite formation of Al_2O_3–SiO_2 gels", J. Mater. Sci., Vol. 29, 1994, pp. 1558.
26. Y. X. Huang, A. M. R. Senos, J. Rocha, J. L. Baptista, "Gel formation in mullite precursors obtained via tetra ethyl orthosilicate (TEOS) pre-hydrolysis", J. Mater. Sci., Vol. 32, 1997, pp. 105.
27. A. K. Chakraborty, S. Das, "Al–Si spinel phase formation in diphasic mullite gels", Ceram. Int., Vol. 29, 2003, pp. 27.
28. H. Kao, W. Wei, "Kinetics and Microstructural Evolution of Heterogeneous Transformation of θ-Alumina to α-Alumina", J. Am. Ceram. Soc., Vol. 83, No. 2, 2000, pp. 362-368.
29. F. Rouquerol, J. Rouquerol, K. Sing, Adsorption by Powders and Porous Solids, ACADEMIC PRESS, London, 1999, pp. 440-441.
30. S. A. Hassanzadeh-Tabrizi, E. Taheri-Nassaj, "Sol–gel synthesis and characterization of Al_2O_3–CeO_2 composite nanopowder", J. Alloy. Compd., Vol. 494, 2010, pp. 289-294.
31. A. Sedaghat, E. Taheri-Nassaj, R. Naghizadeh, "An alumina mat with a nano microstructure prepared by centrifugal spinning method", J. Non-Cryst. Solids, Vol. 352, 2006, pp. 2818-2828.
32. S. J. Gregg, K. S. W. Sing, Adsorption, Surface Area and Porosity, ACADEMIC PRESS, London, 1982, pp. 35